



Applications of Simulation Modeling and Computer Visualizations for Studying Structured Crystals for Implementation in Technical Devices

Yoana Ivanova^(✉)

New Bulgarian University, 21 Montevideo Street, 1618 Sofia, Bulgaria
yivanova@nbu.bg

Abstract. This paper aims to present an experimental study of structured crystals, which has been realized by the integrated use of software products for assessment and analysis of crystal lattices, as well as the building of their three-dimensional color profiles based on the author's microscopic images with a view to subsequently importing them into agent-based simulation environment models for visualization of crystal growth.

The generated results can contribute to extending previous author's research, united in a methodology for the optimization of structured crystals for telecommunication and scientific-technological applications, in which the object of the microscopic and simulation studies are the quartz crystals and the possibilities of their implementation in technical devices such as quartz filters and resonators.

In the present research the focus is placed on simulation methods for the study of ruby crystals after their preliminary optimization. This approach is justified by their possible applications in laser systems, temperature sensor components of modern 3D printers, and medical devices, which aim to increase the efficiency of industrial processes.

Keywords: synthetic ruby · ruby crystal · ruby laser · simulation modeling · computer visualization

1 Introduction

The advanced methods of conceptual design of technical devices are based on engineering 3D modeling and visualizations, as well as simulation modeling and agent-based visualizations. Practically, agent-based simulation modeling is typically supplemented by interactive visualization, which can be modified through changes in the programming code. In this particular case of simulation modeling and visualization of structured crystals, the focus is on the advantages of using “*MaterialSim Grain Growth Model*” [1, 2] for studying the growth of ruby crystals based on the author's microscopic images taken using a digital microscope Levenhuk DTX 90. Actually, the size of ruby grains is the main parameter for evaluating their mechanical properties.

In addition to the microscopic images and agent-based visualizations of the ruby crystals, 3D models of their crystal lattices and color profiles are very useful for the assessment and analysis of their physical and optical properties. Therefore, it is recommended that the study of crystals begins with specialized products for simulating their crystal structure such as Diamond 5 [3]. This approach can contribute to the optimization of the ruby crystals at the atomic and molecular level in order to improve the functionalities of the devices in which they are implemented.

In practice, these devices can be 3D modeled and tested individually at the next stage of a comprehensive research. This is another example of the benefits of applying computer graphics in science and engineering, which will be demonstrated in this paper through the realization in a virtual environment of a medical bracelet design concept that integrates various structured crystals.

Section 2 of the article describes the essence and means of implementing a methodology for the optimization of ruby crystals based on related works. Advanced applications of ruby crystals in technical devices, as well as a conceptual design of a specialized device for medicine and security purposes, are presented in Sect. 3.

2 Related Works

The selected software products used to conduct the practical part of the research are evaluated in Table 1 based on their previous use in a methodology for the optimization of structured crystals for technical applications developed by the author and applied in studying quartz crystals for implementation in quartz filters. The main point of Table 1 is to demonstrate that all the products used for the realization of this study provide a high level of visualization, which is the most important requirement for completing the experimental part of the study.

For example, during the preliminary examination of software products, the author used other excellent resources, such as ShelXle and Crystal Maker, to conduct state-of-the-art research, but the widely available versions of these powerful tools have some limitations. The study aims to improve the educational process in the academic field by helping students better understand these scientific areas. Therefore, using free products offers advantages in this context, and their careful selection is one of the key applied contributions of this research.

The software analysis is made according to the following criteria:

- *high quality of the visualizations*: resolution; realism of colors that is important for the visual interpretation of data; informativeness related to the understanding of the main aspects of digital data.
- *reliability of the generated results* – in this specific case, the verification and validation of the generated results can be based on the microscopic method and a digital method for building 3D color profiles using software. In practice, this process can be bidirectional, depending on the input data available. For example, if the microscopic method is used to acquire input data on the structure and colors of the objects, this data can be used to verify the accuracy of the digital 3D color profiles. The comparison between the microscopic images and the color profiles can show agreement and consistency between the two methods and confirm the reliability of the digital results.

Thus, cross-verification and validation between the microscopic method and digital 3D profiling methods can confirm the accuracy and reliability of the data generated by both techniques.

Each of the next subsections of the current section outlines a stage of a unified methodology for optimizing structured crystals that is adapted specifically to ruby crystals for the purposes of this study. There are different variants of the sequence of phases. For example, in one of the scenarios, the simulation in NetLogo 6.4.0 can be completed before or after the construction of the 3D color model in Fiji [4], and the simulation of the ruby crystal lattice can be performed at the first or second stage. This arrangement depends on the priority goals of the researchers. The recommended sequence is presented in Fig. 1.

Table 1. Evaluation of research software products by criteria

| Software | Description | Visualization quality | Reliability |
|---------------------|---|-----------------------|-------------|
| Portable Capture HD | Microscopic image visualization | high | high |
| Diamond 5 | Simulation modeling of crystal structures | high | high |
| NetLogo 6.4.0 | Agent-based simulation modeling | high | high |
| Fiji | 3D color profiling | high | high |

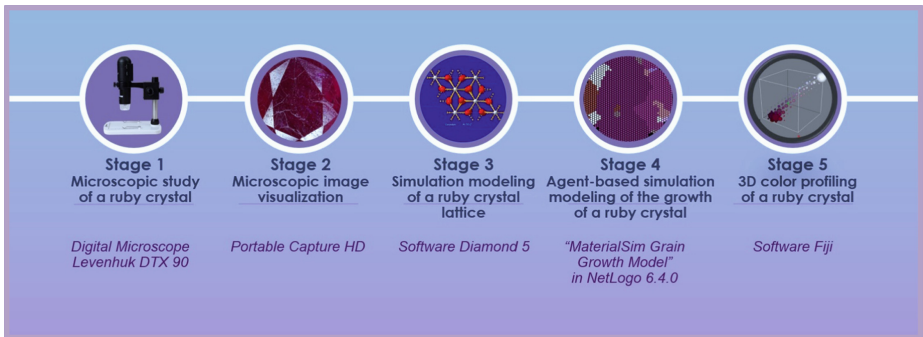


Fig. 1. Stages of a unified methodology for the optimization of ruby crystals.

2.1 A Microscopic Study of a Ruby Crystal

Table 2 presents a comparative analysis of the main types of microscopes that are suitable for the purposes of crystallography by selected criteria, and in particular for the study of ruby crystals, to highlight their advantages and applicability. In the result of the comparative analysis are formulated several conclusions as follows:

- *The principle of operation of a TEM (Transmission Electron Microscope) is expressed in transmitting a beam of electrons through a very thin sample and ensures excellent capabilities for examining ruby crystals in high detail.*
- *The principle of operation of an OM (Optical Microscope) involves passing light through a sample and magnifying the image by using lenses. Actually, it is not very detailed compared to TEM, but it is still suitable for preliminary observation of ruby crystals.*
- *Unlike TEM and OM, the X-ray microscope uses X-rays instead of a light beam or a beam of electrons through a sample, resulting in diffraction patterns that provide information about the crystal lattice arrangement.*

Based on the comparative analysis, it can be concluded that the digital microscope Levenhuk DTX 90, which the author preferred for conducting the experimental study, is characterized by optimal parameters according to the selected criteria. Therefore, it can be highly recommended to users and researchers who are searching for the most balanced combination of functionalities, convenience, and affordability.

Table 2. A classification and comparative analysis of microscopes for studying ruby crystals.

| Microscope type | Magnification | Resolution | Color | Reliability | Availability & safety |
|----------------------|----------------|------------|---------------|-------------|-----------------------|
| OM | 500x–1500x | medium | color | high | high |
| TEM | 50x–5000000x | high | black & white | high | average |
| X-Ray Microscope | Not applicable | high | black & white | high | low |
| DM (Levenhuk DTX 90) | 20x–200x | high | color | high | high |

2.2 A Microscopic Image Visualization

Portable Capture HD offers several significant advantages, including the visualization of microscopic images directly on a computer display as well as the capability to measure object sizes. Figure 2 displays some of the various dimensions of a faceted ruby crystal.

2.3 Simulation Modeling of a Ruby Crystal Lattice

An interesting example of a 3D visualization and 2D diagram generated in Diamond 5 can be illustrated by the “*diffraction diagram*” (from *View Powder Pattern*) shown in Fig. 3. This diagram is a graphical pattern resulting from X-ray diffraction (XRD) conducted on crystals, that contains information about the distribution of the intensity “*Int*” (*I*) of the scattered X-ray radiation, depending on the angle “*Theta*” (θ). In the

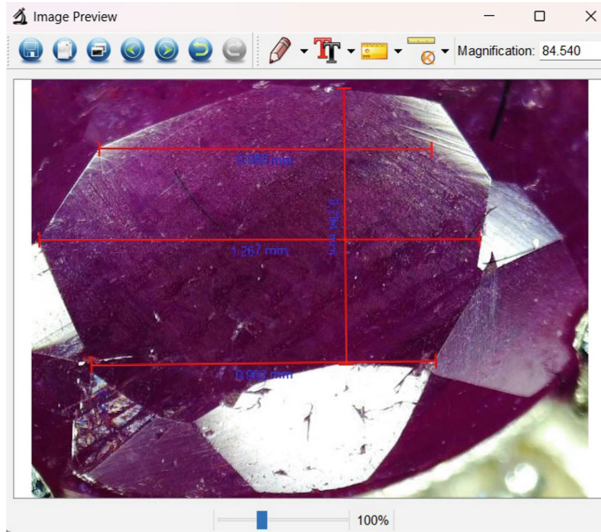


Fig. 2. A microscopic image in Portable Capture HD.

formula for “the intensity of light in a diffraction pattern of a single slit” $\varphi = (\pi a \sin \theta) / \lambda$ and “ a is the location of the first side maximum” [5]:

$$I = I_{max} \frac{\sin^2 \varphi}{\varphi^2} \quad (1)$$

The cell side length of the crystal lattice and the wavelength are measured in \AA (angstroms), with $1 \text{\AA} = 10^{-10} \text{ m} = 0.1 \text{ nm}$. The intensity of peaks is influenced by the atomic number and spatial arrangement of atoms within the unit cell [6]. The unit for measuring the intensity of radiation is “counts per second (cps), which expresses a rate of counts per unit time registered by a radiation monitoring detector” [7, 8], but it is acceptable in the diffraction diagram to be determined as “arbitrary units” [9]. In this case, the simulator calculates this value using embedded algorithms that are based on Bragg’s law:

$$n\lambda = 2d \sin \theta, \quad (2)$$

where d is the “lattice interplanar spacing of the crystal”, n is an integer called “diffraction order”, λ is the wavelength of the X-rays, and “ 2θ ” (2θ) is the scattering angle measured from the incident beam to the scattered beam, considering the deflection of light.

The diffraction diagram illustrates several essential conclusions that follow from Bragg’s law:

- If X-rays strike a crystal lattice at a certain angle (Bragg angle), then constructive interference occurs, resulting in bright diffraction peaks.
- There is a relationship between the Bragg angle, the spacing between the atoms in the lattice, the wavelength of the X-rays, and the diffraction order.

- The positions of the diffraction peaks provide information about the structure of the crystal lattice and especially about the arrangement of the atoms - for example, the maximal peak of the intensity I_{\max} is equal to 458025.88 at $2\theta = 43.378^\circ$.

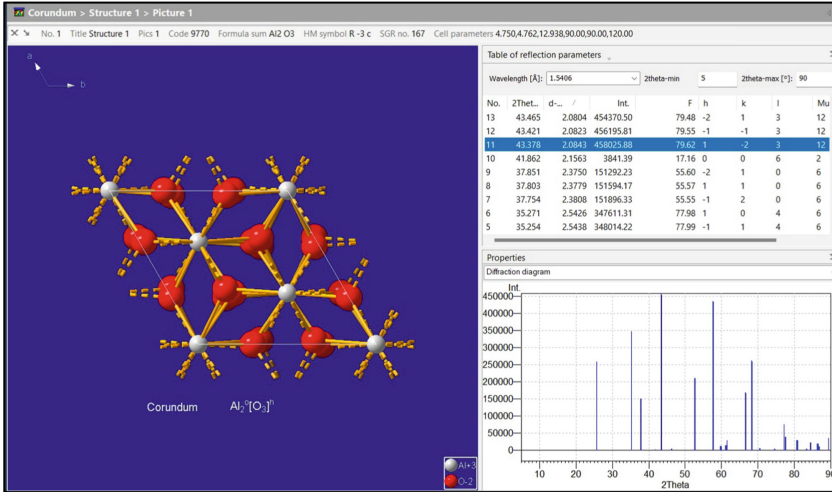


Fig. 3. A 3D visualization of the ruby crystal lattice and a relevant 2D diffraction pattern.

2.4 Agent-Based Simulation Modeling of the Growth of a Ruby Crystal

The screenshot displayed in Fig. 4 presents the simulation results of the referenced at the beginning of the article *MaterialSim Grain Growth model*. The screenshot in Fig. 3 depicts the simulation results of the *MaterialSim Grain Growth model*, which is mentioned at the beginning of the article. It visually depicts the evolution of ruby crystal grain configuration and size over time.

In the demonstrated scenario, the behavior of each individual atom in the system is simulated. Its purpose is to be surrounded by as many atoms as possible with the same orientation as its own. This is done on the principle of random reorientation and finding out if its resistance increases. If it has increased, it remains in its new orientation. Otherwise, the atom should retain its previous orientation. It randomly selects one of its neighbors and navigates in the same direction.

The logarithmic plot accounts for the growth of crystal grains over time, and as an increase in the logarithmic value is observed, this is related to the intensity of the growth. The change in the plots after the period of intense growth should mean that factors such as atomic concentration or structural constraints begin to affect the growth ability of grains that have already reached a certain size.

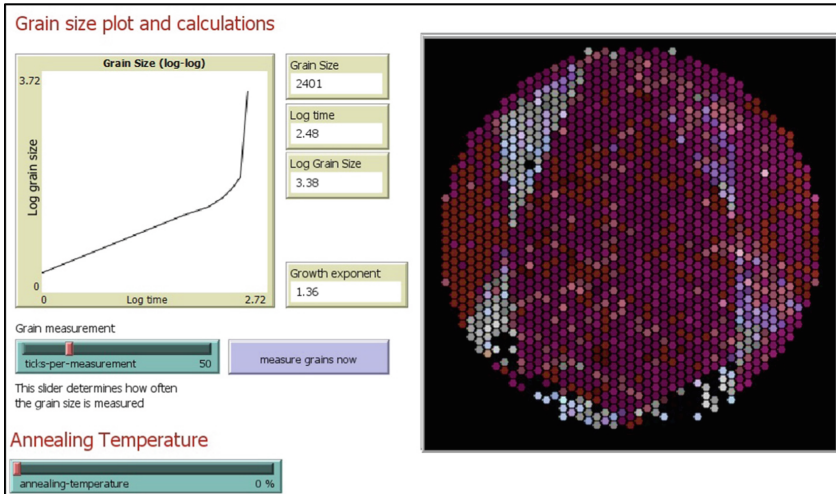


Fig. 4. A logarithmic plot and computer visualization for a microscopic image of a ruby crystal.

2.5 3D Color Profiling of a Ruby Crystal

In Fig. 5, a 3D color profile of a ruby crystal generated in *Fiji* is shown. It is visualized through colored, spherical objects. The colors represent different properties or characteristics of the crystal, which may include, for example, chemical or structural features, defect concentrations, impurities from other minerals, or other parameters that can be analyzed by a visualization.

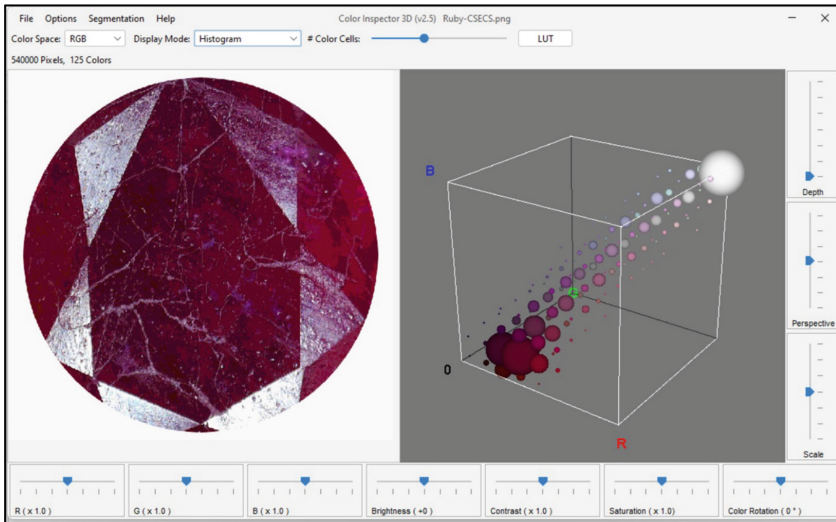


Fig. 5. A 3D color profile of a ruby crystal.

3 Applications of Ruby Crystals in Technical Devices

There are innovative and useful applications of structured crystals in technical devices for the purposes of medical and engineering sciences. Before focusing on the latest technological trends in these areas, it is essential to outline the fundamental role and the main functions of ruby crystals in classical technologies such as ruby lasers. The justification for this necessity is a better understanding of key concepts such as light emission, light, and optical amplification, as well as the technical capabilities and limitations of ruby crystals, respectively.

Medical bracelets are a good example of devices from a new generation, whose intelligent functions pique interest in the fields of medicine, security, defense, and beyond. In practice, their wide use by users of different social statuses, professions, and individual needs is determined by the fact that, in addition to being an innovative and modern accessory, medical bracelets can be qualified as a kind of digital health assistant of primary necessity for every modern user.

The main purpose of medical bracelets is related to measuring physiological parameters (heart rate, blood pressure, and blood oxygen levels), physical activity (burned calories and number of steps), health status (estimation of stress levels), as well as the storage of medical information about the holder (blood type, allergies to substances, and medications). In addition, the innovative human face simulation methods can effectively be used in interactive therapeutic applications, where the emotional state of the patient needs to be diagnosed based on their facial expressions.

It is important to differentiate between medical bracelets and magnetic bracelets, which have also gained popularity since the early 2000s. Magnetic bracelets contain embedded magnetic elements that are believed, in alternative medicine, to positively affect the body. This belief often leads to claims of improved blood flow, muscle relaxation, and relief from mild to moderately painful conditions.

The presented overall concept for the design of a new generation medical bracelet with medical diagnosis capabilities by measuring key health indicators and environmental parameters is a continuation of the author's previous research, in which microscopic, digital, and simulation methods were used for the optimization of structured quartz and ruby crystals for applications in telecommunications, radio electronics, and security.

3.1 Conceptual Design of a Medical Bracelet

The choice of materials is a very important part of conceptual design. In favor of satisfactory results, the materials for making the individual components have been considered both from a practical and aesthetic point of view, as well as from the point of view of their positive impact on the health of users and military personnel. While in quartz watches the main function of the quartz crystal is related to the generation of a stable clock signal, on which the accuracy of the measured time depends, in modern medical bracelets quartz crystals are applied as components of more complex devices, i.e., as part of electrical circuits of frequency regulators or time synchronizers with other devices [10].

In practice, quartz filters and resonators are used for precise time measurement, data synchronization, frequency stabilization of signals, and communication processes

(radio or Bluetooth modules). Under the influence of electric voltage, the quartz resonator vibrates at a constant and stable frequency, which is used as a reference for measuring time. The principle of operation of quartz filters is based on the properties of quartz crystals to respond to certain resonant frequencies, thus blocking unwanted or missing frequencies required for specific applications. This makes these electronic devices useful for implementation in sensor and communication systems. It should be emphasized that regardless of the specific purpose, in view of the accuracy of the measurement of parameters in quartz devices, the implementation of synthetic crystals is preferred due to their purity [11].

Combining materials with magnetic properties with technical devices (such as sensors) in a medical bracelet is achievable by meeting certain technical requirements, which can prevent unwanted interference on the sensor electronics due to magnetic fields. Shielding materials or magnetic insulators can be used for this purpose to minimize the impact of external magnetic fields on the measuring devices. The choice of suitable shielding materials is determined by the type of shielding needed.

In magnetostatic shielding, ferromagnetic materials (manganese-zinc ferrites, nickel-zinc ferrites, lithium ferrites, etc.). Placing them around the sensitive devices protects them by absorbing the magnetic waves and, respectively, reducing the induction on the sensitive devices. Aluminum, copper, and bronze metals are suitable for shielding high-frequency electromagnetic waves, as they can divert currents flowing through them from electronic devices [12]. In this way, the devices are protected from electromagnetic interference due to communication signals, radio waves, etc. In terms of measuring devices, combining several functionalities can be useful, such as, for example, the “*Adafruit BME280 combined air temperature, pressure, and humidity sensor and DS3231- based hardware clock*” [13].

3.2 Building a 3D Model and Visualization of a Medical Bracelet with Implemented Crystals

The first stage of the realization of the device is the construction of an engineering 3D model, which is not only informative from the point of view of the location and connection of the individual components in the overall device but also enables some of them to be subsequently printed with a 3D printer from suitable materials (metals, resins, sustainable and ecological plastics), as well as in different sizes according to the individual characteristics of a specific user.

The engineering model of the basic load-bearing components of the medical bracelet is initially constructed using specialized engineering 3D modeling software, Autodesk 123D Design. The model was subsequently upgraded in the professional 3D virtual environment design software Autodesk 3DS Max, which is suitable for modeling components that are crucial not only for the functional implementation of the device but also for its visualization in a virtual environment. It is necessary to note that the implementation of crystals in the medicine bracelet contributes to its stylish appearance as an additional effect, but its main purpose is to add useful functionalities.

In Fig. 6, screenshots taken during engineering modeling in Autodesk 123D Design software are presented, while a basic functional prototype of the bracelet printed using a 3D printer “*da Vinci mini w+*” and connected to Epson MOVERIO Augmented Reality

Smart Glasses is shown in Fig. 7. The orientational sizes of the bracelet depicted in the drawings are in centimeters, although its dimensions may vary depending on the individual characteristics of the user and are not critically important. These screenshots illustrate the accuracy of the model. The main requirements for the bracelet are the preferences and convenience of the user. Table 3 provides example sizes for clarity, which can be adjusted using 3D printer software as needed.

Table 3. Bracelet size guidelines by categories.

| User category | Length range, cm | Width range, cm |
|----------------------|------------------|-----------------|
| Children (7 + years) | 14–16 | 1–2 |
| Male | 18–20 | 2–5 |
| Female | 16–18 | 2–4 |

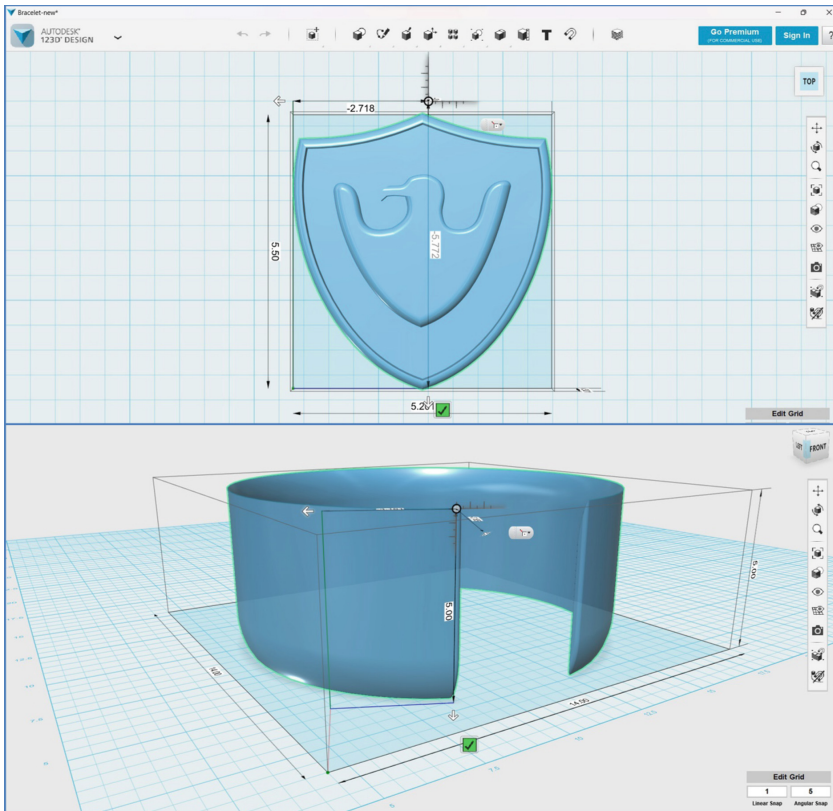


Fig. 6. Engineering modeling of a medical bracelet in Autodesk 123D Design software.



Fig. 7. A 3D printed bracelet connected to a virtual reality system Epson MOVERIO Augmented Reality Smart Glasses.

The style of the bracelet is classic, with the design consciously incorporating specific components recognizable to consumers from the specific target group for which the product would be useful. It is important to note that it is impossible to create a design that perfectly aligns with the individual preferences of every potential user. However, the design solution for the emblem includes separate components with key symbolic values.

In addition to better describing the accuracy of the 3D model, Fig. 8 presents two screenshots taken during the modeling process in Autodesk 3DS Max. Figures 9, 10, 11, and 12, the final rendered images of the 3D model, depicting the overall composition of the scene with added textures, materials, and lighting.

In fact, the abstraction of a shield is associated with protection and security in all its aspects, while the eagle or falcon are preferred symbols of strength, power, freedom, and superiority, which is why they are mainly used by the Air Force of various countries. But in general, the design of the bracelet is suitable for men and women, who can also be civilians, if they have a need for a device with such functions. In the fourth image, for the texture of the display of the main unit, the Apple interface is used [14].

Actually, the device utilizes synthetic quartz and ruby crystals in specific components to improve measurement precision and enable practical applications in security contexts. The clasp mechanism, as recommended by the author, can be crafted from bracelet properties such as mineral magnetite, which is applied to the shield in the 3D model. To ensure comfort and safety, the bracelet can feature a metal core lined with leather to prevent discomfort, injuries, and allergic reactions, especially in low temperatures. Thanks to this, it should not be lost even without the additional protection provided by the closing mechanism.

In practice, the magnetite component is characterized by multifunctionality, serving simultaneously to regulate a number of health indicators in the body and as a supporting part for the ruby temperature sensor and the eagle decoration, which serves to shield the sensor electronics in order to prevent possible interference during measurements under the influence of magnetite.

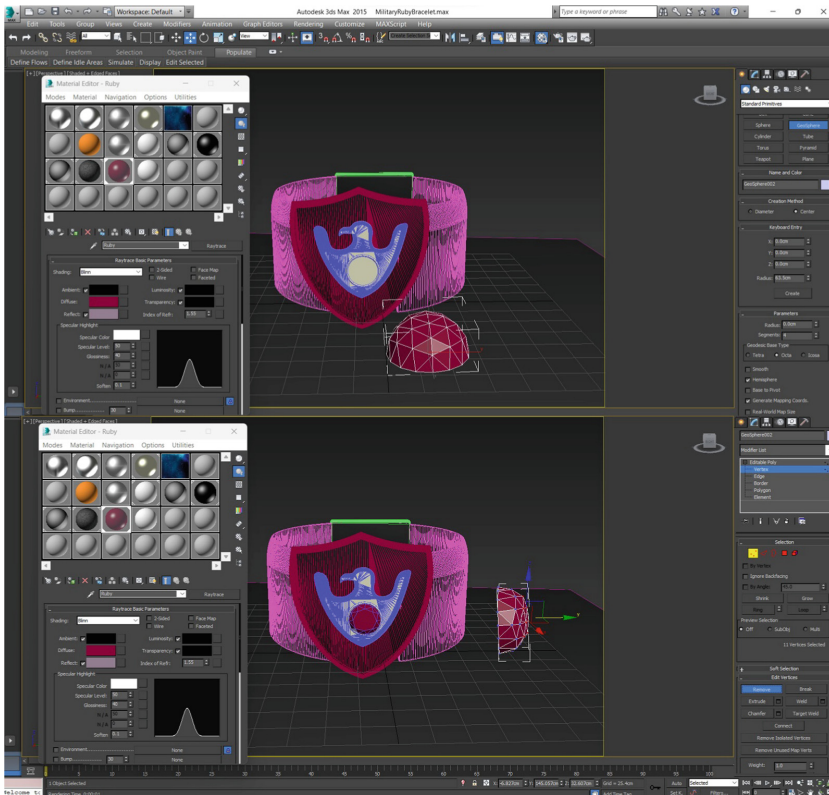


Fig. 8. Screenshots taken during the modeling process in Autodesk 3DS Max, illustrating the techniques for achieving the realism in the visualization.

Last but not least, it is important to explain the meaning of the chosen name of the *MaxiMedic RubyMag* medical bracelet. The first part of it aims to draw attention to the maximum medical abilities that are embedded in it (“*maxim*”, an abbreviation of the English “*maximum*” and the word “*medic*” in the sense of paramedic, healing). The idea for the second part of the name includes the names of two of the main minerals in the clasp mechanism (“*ruby*”—ruby and *mag*—short for “magnetite”).



Fig. 9. A rendered image of the scene created in Autodesk 3DS Max in the front viewport.



Fig. 10. A rendered image of the scene created in Autodesk 3DS Max in the left viewport.

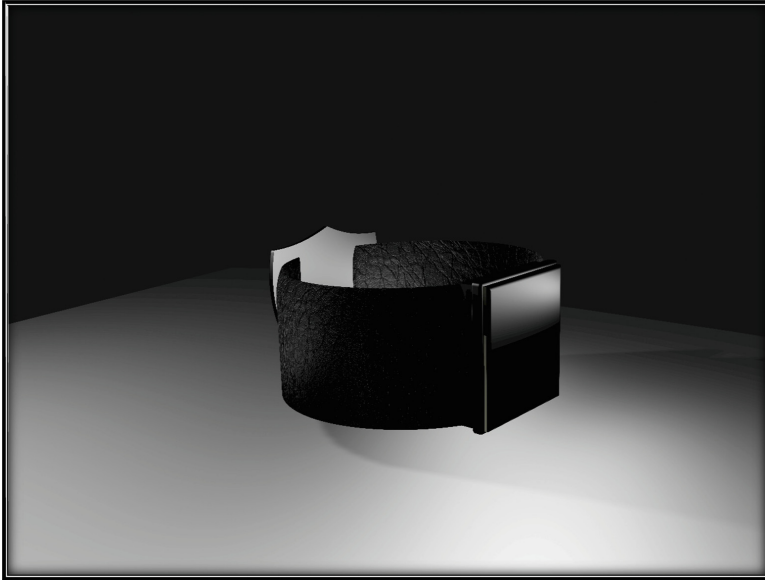


Fig. 11. A rendered image of the scene created in Autodesk 3DS Max in the right viewport.

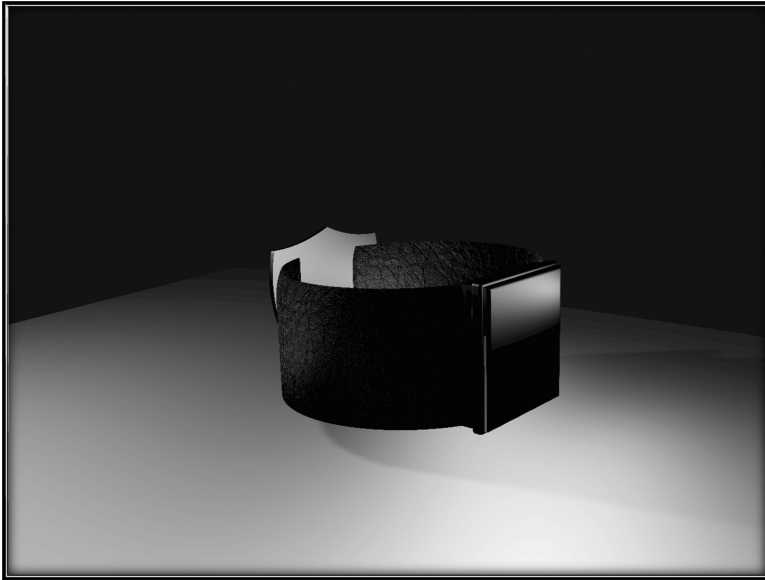


Fig. 12. A rendered image of the scene created in Autodesk 3DS Max in the perspective viewport.

4 Conclusion

The described in the paper integrated approach for studying ruby crystal structures built upon a previously established methodology for optimization of quartz crystals contributes to a deeper understanding of their optical (double refraction), physical (thermal conductivity) and chemical properties (stability) [15] in order to be effectively implemented in technical devices for various applications in engineering, medical sciences, and security. In addition, simulation modeling combined with 3D computer graphics is a powerful tool for visualization of processes in the crystal lattice. Moreover, 3D modeling is very useful for preliminary developing design concepts of technical devices enabling simulation for the enhancement of their functionalities.

In conclusion, it can be summarized that medical bracelets can significantly improve the quality of life, providing prerequisites and conditions for strengthening the health status, especially for groups of users who are exposed to the potential risk of life-threatening situations. Apart from the functionalities provided, their value is determined by the materials of manufacture. The selection of materials that have specific properties can add new functionalities to the medical device, which can significantly contribute to maintaining the good health of users.

References

1. Blikstein, P., Wilensky, U.: NetLogo MaterialSim Grain Growth model, Center for Connected Learning and Computer-Based Modeling, Northwestern University, Evanston, IL (2005). <http://ccl.northwestern.edu/netlogo/models/MaterialSimGrainGrowth>
2. Wilensky, U.: NetLogo, Center for Connected Learning and Computer-Based Modeling, Northwestern University, Evanston, IL (1999). <http://ccl.northwestern.edu/netlogo/>
3. Crystal Impact, DIAMOND Crystal and Molecular Structure Visualization, User Manual, Version 4.6 [Online], chrome-extension://gphandlahdpffmccakmbngmbjnjiiiahp/<https://www.crystalimpact.com/download/diamond4/manual.pdf>. Accessed 25 Apr 2024
4. Fiji <https://fiji.sc/>. Accessed 25 Apr 2024
5. Chegg, Question: 52. The intensity of light in a diffraction pattern... <https://www.chegg.com/homework-help/questions-and-answers/52-intensity-light-diffraction-pattern-single-slit-described-equation-sin2-max-0-side-maxi-q38750085>. Accessed 26 Apr 2024
6. Rutgers Physics, Crystal Structure Analysis, chrome-extension://gphandlahdpffmccakmbngmbjnjiiiahp/<https://www.physics.rutgers.edu/~eandrei/389/xrays/exp.pdf>. Accessed 26 Apr 2024
7. Nuclear Power for Everybody, Counts per Second – CPS. <https://www.nuclearpower.com/nuclear-engineering/radiation-detection/detectors-of-ionization-radiation/counts-per-second-cps/>. Accessed 26 Apr 2024
8. Uz, V., Uz, B., Issi, A., Coşkun, N.D., Yıldız, T.D.: The Annealing of Corundum (Ruby) in Nitrogen (N₂) Air, El-Cezeri Fen ve Mühendislik Dergisi **5**(3), 875–881 (2018). <https://doi.org/10.31202/ecjse.436515>
9. Dong, H., Dorfman, S.M., Wang, J., He, D., Duffy, T.S.: The strength of ruby from X-ray diffraction under non-hydrostatic compression to 68 GPa. Phys. Chem. Miner. 527–535. Springer-Verlag Berlin Heidelberg (2014). ISSN: 0342-1791. <https://doi.org/10.1007/s00269-014-0664-2>

10. Quartz Crystal Filter Design, Equivalent Circuit Determination of Quartz Crystals. https://www.changpuak.ch/electronics/Quartz_Crystal_Filter_Designer_1.php. Accessed 27 Apr 2024
11. Spasov, L.: Visokochuvstvitelni kvartsovi temperaturni senzori, Treti natsionalen kongres po fizicheski nauki, 29 septemvri – 2 oktomvri 2016 g., Heron Pres Sofia (2016). ISBN 978–954–580–364–2
12. WikipediA, Dielektrichna konstanta. https://bg.wikipedia.org/wiki/Dielektrichna_konstanta. Accessed 27 Apr 2024
13. Adafruit, Adafruit BME280 Humidity + Barometric Pressure + Temperature Sensor Breakout. https://learn.adafruit.com/adafruit-bme280-humidity-barometric-pressure-temperature-sensor-breakout?view=all&gad_source=1&gclid=CjwKCAjwxLKxBhA7EiwAXOOR0EZfIIFIHAj7eLZ8RQtcstp5Of1-rcWjblrLLKzGsPIDPWT6avr2WBoCrW8QAvD_BwE. Accessed 27 Apr 2024
14. Apple, Monitor your heart rate with Apple Watch. <https://support.apple.com/en-ca/HT204666>. Accessed 27 Apr 2024
15. Yang, L., Lu, Q., Ma, D., et al.: Chemical composition and spectroscopic characteristics of heat-treated rubies from madagascar. Mozambique Tanzania Cryst. **13**(7), 1051 (2023). <https://doi.org/10.3390/cryst13071051>